J Solid State Electrochem (1999) 3: 437–445

ORIGINAL PAPER

Stefan Rysy · Horst Sadowski · Reinhard Helbig

Electrochemical etching of silicon carbide

Received: 29 October 1998 / Accepted: 27 January 1999

Abstract Both n- and p-type SiC of different doping levels were electrochemically etched by HF. The etch rate (up to 1.5 μm/min) and the surface morphology of p-type 6H-SiC were sensitive to the applied voltage and the HF concentration. The electrochemical valence of 6.3 ± 0.5 elementary charge per SiC molecule was determined. At p-n junctions (p-type layer on a n-type 6H-SiC substrate) a selective etching of the p-type epilayer could be achieved. For a planar 6H-4H polytype junction (n-type, both polytypes with equal doping concentrations) the 4H region was selectively etched under UV illumination. Thus polytype junctions could be marked by electrochemical etching. With HCl instead of HF no etching of SiC occurs, but a SiO_2 layer (thickness up to 8 μm) is formed by anodic oxidation.

Key words Electrochemical etching · Silicon carbide · p-n junction · Polytype · Anodic oxidation

Introduction

SiC is a promising semiconductor material for electronic devices operating under extreme conditions (e.g. high temperature, high frequency and high power). Furthermore, there exist more than 200 different crystal modifications [1], so-called polytypes mostly with different energy gaps, suggesting the development of polytype heterojunction devices, e.g. polytype heterojunction bipolar transistors made of one chemically identical material.

The processing of electronic devices made of the hard and chemically inert SiC demands suitable etching methods. So far, the most effective method is reactive ion etching (RIE), which gives satisfying results in producing smooth surfaces and in forming mesa structures [2] (review is available by Yih et al. [3]). Etching by molten alkali hydroxides (e.g. KOH) is mainly used for the decoration of defects like pinholes and dislocations [4]. However, none of these conventional etching methods shows any selectivity concerning conductivity type or polytype, in contrast to electrochemical etching [5, 6]. We present in this paper that etching rates during an electrochemical etching process depend on both the conductivity type and the polytype. This way it may be possible to structure both bipolar and heteropolytype devices.

In previous studies on electrochemical etching of SiC, mainly the polytypes 3C and 6H were studied by electrochemical etching, leading to a variety of results including electropolishing or mesa structuring [7]. Few reports exist about the etching of p-type 6H-SiC [8, 9]. We know of two studies which examined the etching of p-n junctions, observing an etch stop at the p-n junction, one using 3C-SiC [5], the other using 6H-SiC [6]. In both cases, an n-type epilayer was selectively etched, while the underlying p-SiC remained inert. We do not know of previous studies concerning the etching of SiC polytype heterojunctions.

Experimental

For the etching process we used an electrochemical cell made of Teflon, as shown in Fig. 1. The SiC sample to be etched was mounted in a hollow at the bottom of the cell. The specification of the SiC samples are given in the different sections below. The SiC sample was pressed against an O-ring seal (inner diameter 1.78 mm or 3.00 mm) defining a circular area on the surface of the sample which was exposed to the electrolyte solution. The etched area is determined additionally by considerable "under-etching". To form an ohmic contact at the back side of the sample, a thin Pt foil was pressed against the sample and conductively connected by a Ga/In eutectic.

The electrolyte solution consisted of dilute HF between 1 M and 4 M, corresponding to different volume ratios of 50% HF:H_2O:ethanol (1:19:10 for 1 M HF, 4:16:10 for 4 M HF). By a

S. Rysy · H. Sadowski (✉) · R. Helbig
Institute of Applied Physics,
University of Erlangen-Nürnberg,
Staudtstrasse 7/A3,
D-91058 Erlangen, Germany
e-mail: mpap05@rzmail.uni-erlangen.de

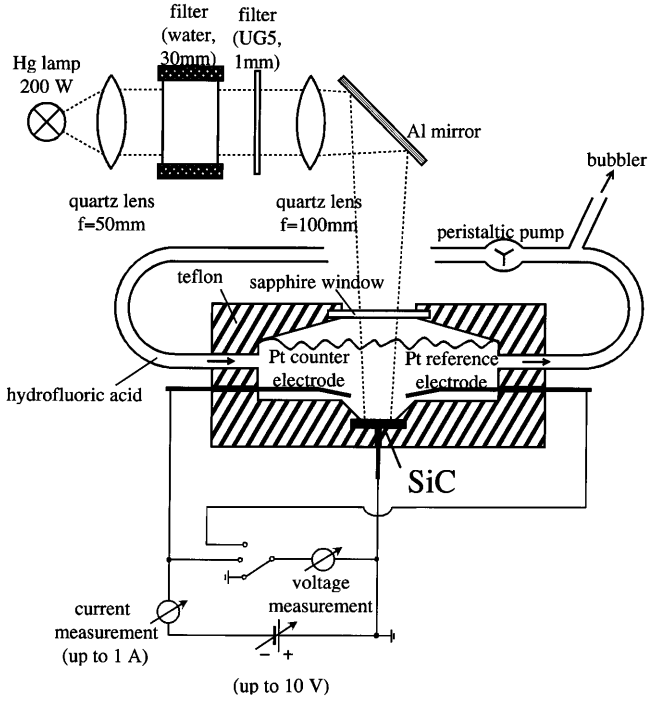

Fig. 1 Scheme of the apparatus used for electrochemical etching of SiC

peristaltic pump the solution was circulated to avoid heating and inhomogeneities in the electrolyte. During particular etching procedures, the SiC was illuminated by a 200 W Hg arc lamp. Filters (Schott UG5, deionized water) selected light of the spectral range of 250–400 nm wavelength, resulting in a power density of 1 W/cm^2 on the sample surface. Etching was performed at constant voltage conditions (up to 10 V). The SiC sample was used as an anode, a Pt wire served as a counter electrode, another Pt wire as a reference electrode[1]. After the etching procedure, the generated structures were examined by a profilometer (Veeco Dektak 3030ST), by light microscopy and by photoluminescence.

Mechanism of electrochemical etching

The etching process can be separated into two steps. In a first step the electric current through the interface SiC electrolyte solution results in the oxidation of the SiC as described by the following reaction equations [10] (h^+ means the positive charge transfer by a "hole"):

$$SiC + 2H_2O + 4h^+ \Rightarrow SiO + CO\uparrow + 4H^+ \quad (1)$$

$$SiC + 4H_2O + 8h^+ \Rightarrow SiO_2 + CO_2\uparrow + 8H^+ \quad (2)$$

In a second step the oxide has to be removed by HF contained in the electrolyte solution [11]:

$$SiO_2 + 6HF \Rightarrow 2H^+ + SiF_6^{2-} + 2H_2O \quad (3)$$

For energetic reasons [12] the electrochemical etching of SiC is driven by holes as charge carriers. Therefore, the etching of p-type and n-type SiC has to be conducted by different procedures, as will be explained below.

To understand the different etching mechanisms of p-type and n-type SiC, it is necessary to consider the electronic energies at the SiC-electrolyte interface, which are similar to those at a Schottky contact. Figure 2a shows the energy band diagram at the interface in the case of p-type SiC without applied voltage V. Since the Fermi level E_F of SiC and the redox energy E_{redox} of the HF match at equilibrium, the SiC energy bands are bent downwards at the interface, causing holes to be driven into the bulk and therefore creating a space charge region. Thus no etching is possible. If a positive voltage is applied (i.e. the SiC is anodically polarized), E_F shifts downwards and the energy bands become flatter or even bend upwards. Figure 2b shows the flat-band situation, characterized by the flat-band voltage V_{fb}. If $V \geq V_{fb}$, no potential detains the holes from moving to the interface and, therefore, etching is possible. The j-V characteristics of p-type SiC reflects this mechanism (see Fig. 3), showing a threshold voltage of about 1.5 V.

The situation is different for n-type SiC, as the energy band diagram in Fig. 4 (without applied voltage V)

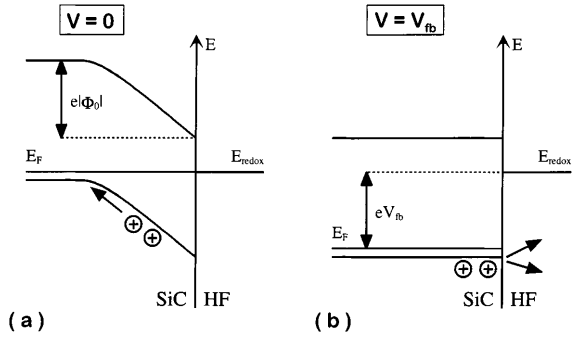

Fig. 2 Energy band diagram of p-type SiC in HF with different applied voltages V: **a** $V = 0$: depletion of holes; no etching; **b** $V = V_{fb}$: flat-band situation; holes are reaching the surface; etching is possible

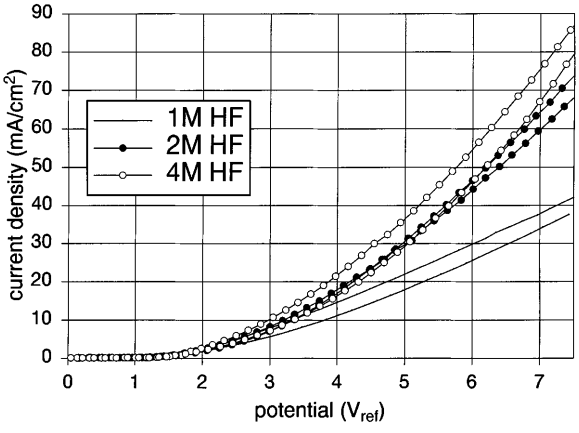

Fig. 3 j-V characteristics of a p-type SiC sample (6H, N_A-$N_D = 7 \times 10^{17}$ cm^{-3}) in different HF electrolytes of different concentrations

[1] Here could be a source of an error because we have not controlled the electrode process at the reference electrode

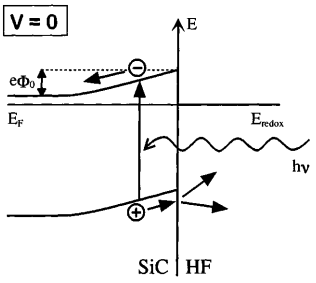

Fig. 4 Energy band diagram of n-type SiC in HF without an applied voltage V. A photon generates an electron-hole pair; etching is possible

displays. The SiC energy bands are bent upwards, driving holes towards the interface. Since their concentration as minority charge carriers is negligible, the SiC has to be illuminated by UV light, generating electron-hole pairs which are separated in the space charge region (see Fig. 4) and, therefore, etching is enabled. Figure 5 shows the j-V characteristics of n-type SiC. Without illumination (filled triangles), no current flows and no etching occurs. With UV illumination (open triangles), current can be observed even at 0 V. During the etching process, however, the current decreases drastically, which is attributed to the formation of a passivating surface layer of porous SiC [6].

These different mechanisms enable selective etching of p-type and n-type SiC by a suitable choice of etching conditions.

Results on p-type SiC

Etching results of a p-type SiC sample (bulk material from Cree, 6H, C-face) are presented. The sample showed a doping level of 7×10^{17} cm^{-3} and a surface roughness of 3 nm. Etching was performed on nine spots, using HF concentrations between 1 M and 4 M and voltages between 2 V and 8 V (vs. reference electrode). These voltages are higher than the flat-band voltage, as the j-V characteristics of this sample show (Fig. 3). Each spot was etched for 40 min at a constant voltage.

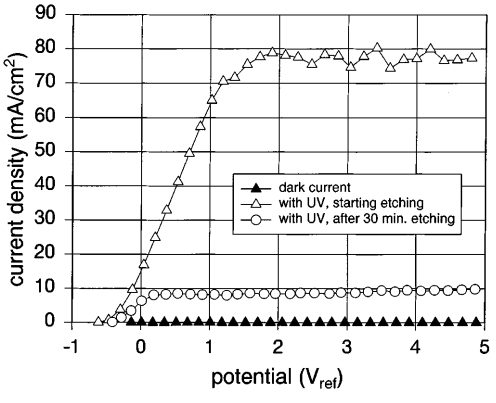

Fig. 5 j-V characteristics of a n-type SiC sample (6H, $N_D = 7 \times 10^{17}$ cm^{-3}) in 2 M HF, with and without UV illumination, starting and after 30 min of etching

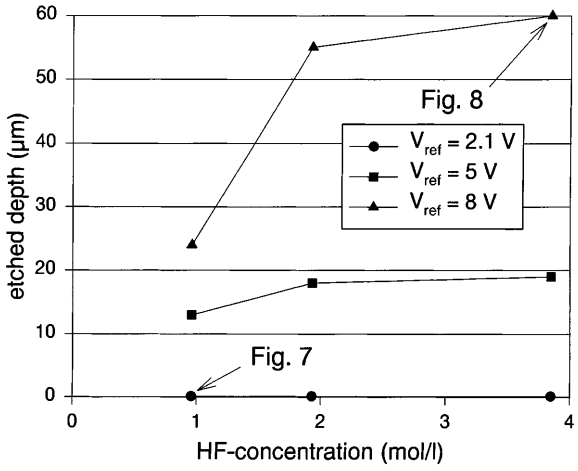

Fig. 6 Dependence of the etched depth of a p-type sample on the HF concentration for different reference bias voltages (etching time: 40 min)

Each etching experiment produced a distinct trough with a diameter of about 2.3 mm (inner O-ring diameter: 1.78 mm). Both depth and morphology of the trough depend drastically on the parameters used. The survey of the etched depths in Fig. 6 illustrates the dependence of the etch rate on the HF concentration and the applied voltage. To demonstrate this dependence, two of the etched structures (marked in Fig. 6) are examined in detail.

Low HF concentration (≤1 M) and low voltages (2.1 V and 5 V) and thus low etch rates result in a smooth surface. Figure 7 shows the depth profile of such a structure (1 M HF, 2.1 V) with a depth of 100 nm and a surface roughness of 4 nm. This roughness is about the same as prior to the etching step. The shiny and uniform appearance of the surface remains after etching. The spikes in the depth profile are due to dust particles.

Higher HF concentration and higher voltage cause a higher etch rate. In Fig. 8 (4 M HF, 8 V) a depth of 60 µm is etched, corresponding to an etch rate of 1.5 µm/min. This leads to the formation of etch pits at

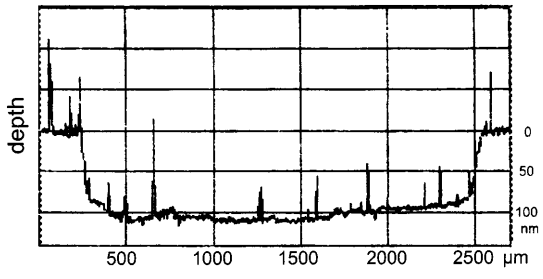

Fig. 7 Profilometer measurement of the etched depth of an etched p-type sample with 1 M HF, $V_{ref} = 2.1$ V. *Spikes* are due to dust particles

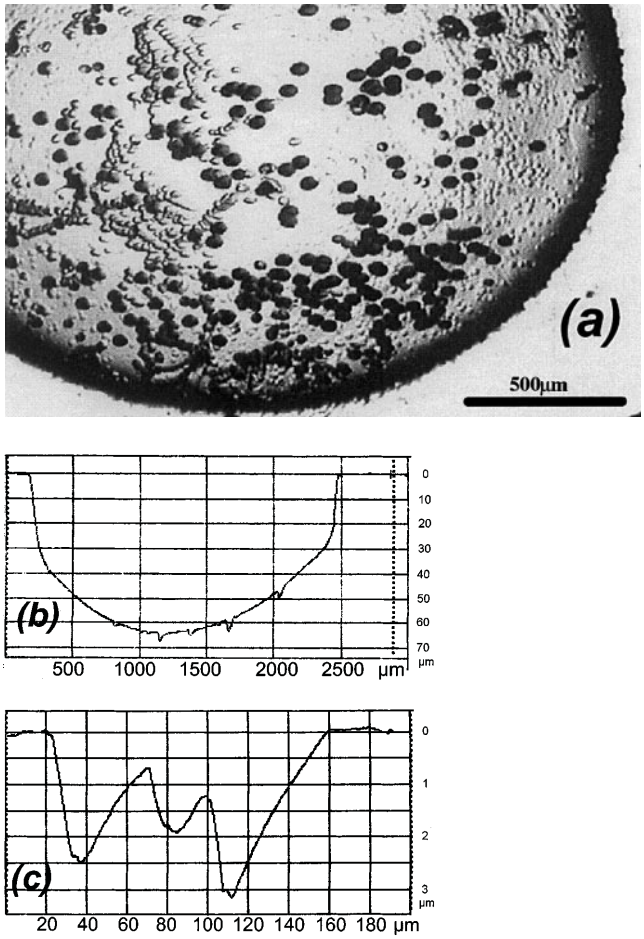

Fig. 8 An etched p-type sample with 4 M HF, $V_{ref} = 8.2$ V **a** optical microscope picture of the etched region with etch pits; **b** profilometer measurement of the etched depth of this region with troughs; **c** profilometer measurement of the etched depth (expanded scale) of a single trough

the bottom of the trough, as the microscopic picture (Fig. 8a) shows. The profile in Fig. 8c displays a detail of the bottom of the trough. It reveals that the etch pits are conical in shape and 2–3 µm in depth. Their size depends on the etching parameters.

Equation 1 (leading to bivalent oxidation products) and Eq. 2 (leading to quadrivalent oxidation products) are the two extreme possibilities of the oxidation process of SiC. Information about the real reaction equation is provided by the electrochemical valence Z_{SiC}. The electrochemical valence Z_{SiC} is defined as the ratio of the number of consumed elementary charges N_e to the number of etched SiC molecules N_{SiC}. The value of the electrochemical valence Z_{SiC} must be between 4 (Eq. 1) and 8 (Eq. 2). For the discussed series of etching processes, the value of the electrochemical valence Z_{SiC} could be determined experimentally:

$$Z_{SiC} = \frac{N_e}{N_{SiC}} = \frac{Q/e}{\Delta m / m_{SiC-molecule}} \quad (4)$$

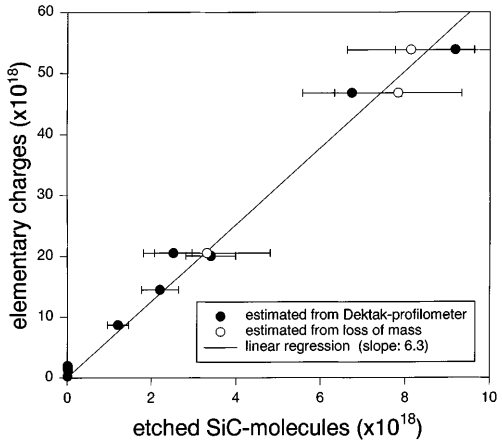

Fig. 9 Measured dependence between flow amount of elementary charges and etched SiC molecules of a p-type sample

Figure 9 shows N_e as a function of N_{SiC} for nine etching experiments. N_e was obtained from the measured charge flow Q. N_{SiC} was obtained either from the loss of mass Δm of the sample (white dots in Fig. 9) or from the volume of the etched trough, which is estimated from the etch profile (black dots in Fig. 9). A straight line was fitted to the experimental values, whose slope of 6.30 ± 0.51 represents the electrochemical valence Z_{SiC}.

Discussion

Both HF concentration and applied voltage strongly influence the etch rate and the surface morphology of the etched sample. It is possible to vary between electropolishing and the decoration of defects by selecting appropriate parameters. The preferred etching of defects can be explained in the case of an excess concentration of HF, where etching is limited by the supply of holes. Small deepenings locally focus the electric field and therefore the hole and etch pits are formed. However, it is not clear if the etch pits decorate dislocations or pinholes. Dislocations etched in molten alkali hydroxides cause hexagonal etch pits, whereas electrochemical etching produces only conical etch pits, which was also reported before [9]. It seems that an easy way to obtain crystallographic orientation of SiC samples – by orientation of etch pits produced by electrochemical etching – is not possible.

The obtained value of 6.30 ± 0.51 elementary charge for the electrochemical valence of p-type SiC is comparable to previously reported values for n-type SiC [13, 14]. This indicates that the electrochemical valence and thus the nature of the oxidation products are independent of the doping type. The value of about 6 means that the real reaction process is a mixture between Eq. 1 and Eq. 2. Since the electrochemical oxidation without dissolution using HCl instead of HF generates an oxide with a stoichiometry close to SiO_2, carbon seems to be oxidized preferably to CO instead of CO_2.

Results on p-n junctions

For investigating the etching of p-n junctions, three different designs of p-n junctions (polytype: 6H) were used. Some samples were prepared as p^+pn^+-mesa diodes (see Fig. 10a) and n^+np^+-mesa diodes (see Fig. 10b) kindly supplied by the INSA Institute in Lyon, France, and made by Cree. One sample prepared by Al implantation is a planar p-type structure in a n-type substrate (see Fig. 10c). All measurements on samples with the p-type epilayer on top were conducted under reverse bias of the p-n junction; samples with the n-type epilayer on top were etched under forward bias.

p^+pn^+-mesa diodes

The p-type CVD epilayer and the n^+-CVD epilayer have a doping concentration of 1×10^{16} cm^{-3} and 1×10^{19} cm^{-3}, respectively. The structure of the mesa diodes was produced by RIE. The height of the mesa structure is about 3.4 μm; the diameter varies from 0.1 mm to 1.2 mm. In every etching process, several diodes were placed within the O-ring seal. Under UV illumination with 4 M HF using a bias of 2 V on both Pt electrodes, the same region was etched four times with a total duration of 94 min.

Figure 11 shows a scanning electron microscope image of a non-etched diode and one of an etched diode, respectively. The different doping concentrations can be distinguished by the different grey steps. The wall of the non-etched mesa diode is smooth, showing vertical lines produced by the RIE process (Fig. 11a). The wall of the electrochemical etched mesa diode shows two different slopes: the p-base reveals a higher slope than the n-type layer; the RIE-lines are missing (Fig. 11b). The ratio of the thickness of the n-type layer to the p-type base underneath also varies between the etched and the non-etched diode. Profilometer measurements show that the height of the mesa diode itself has grown from 3.4 μm to 3.8 μm (Fig. 12). Therefore, the p-type base has been etched preferably. This result was reproduced also without any UV illumination.

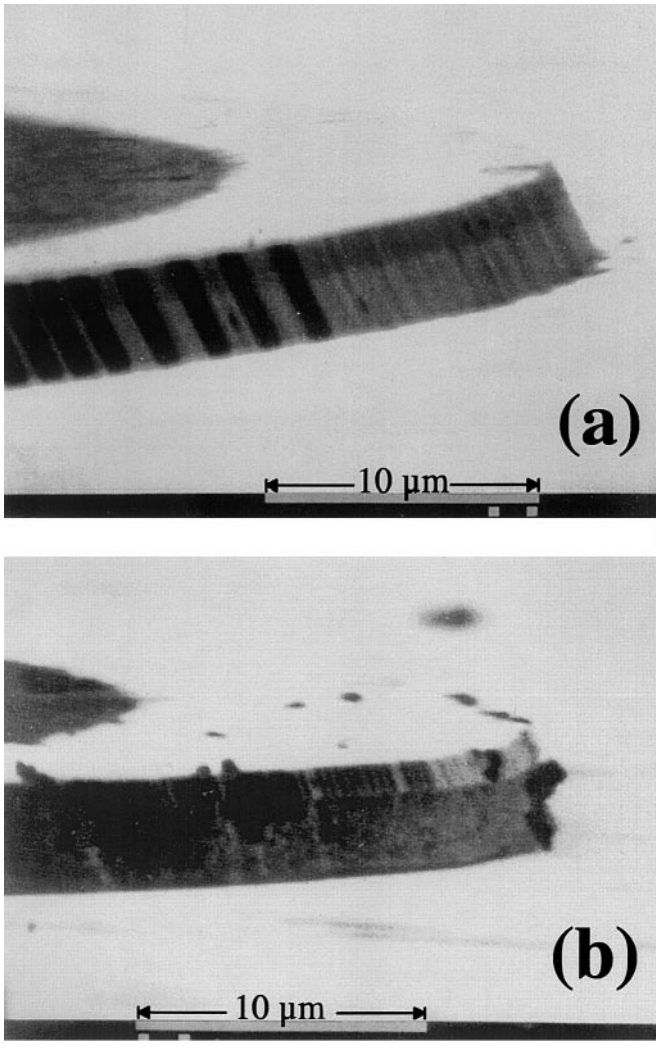

Fig. 11 Scanning electron microscope (SEM) picture of a p^+pn^+-mesa diode. The different n- and p-type regions are distinguished by the different grey steps: **a** before etching process; **b** after etching

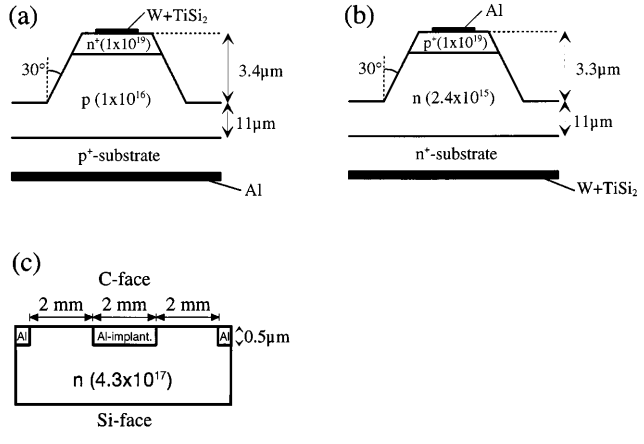

Fig. 10 Scheme and parameters of the used different p-n-junctions: **a** p^+pn^+-mesa diode; **b** n^+np^+-mesa diode; **c** ion implanted p-type region in n-type substrate

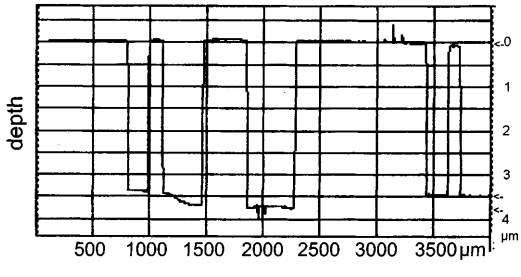

Fig. 12 Profilometer measurement of the etched depth of p^+pn^+-mesa diodes after the etching process. Only the p-base is etched. The bottom between the first two diodes on the left was located under the O-ring and is not etched

Table 1 Etching results of the ion implanted p-type SiC sample

UV illumination	V_{ref} (V)	Etching time (min)	Result
Yes	−0.15	10	different etching of n- and p-type region
Yes	−0.12	10	different etching of n- and p-type region
Yes	−0.12	10	different etching of n- and p-type region
Yes	+0.15	2	only etching of p-type region; etch stop
Yes	+0.16	20	only etching of p-type region; etch stop
Yes	+0.20	20	only etching of p-type region; etch stop
No	+5.3	10	no etching
No	+8.7	10	no etching

Ion implanted sample

The implanted p-type region has a box-like concentration profile with an aluminum concentration of 5×10^{18} cm^{-3} and a thickness of about 0.5 μm; the doping concentration of the n-type substrate is 4.3×10^{17} cm^{-3}. A part of the p-type region as well as a part of the n-type substrate were located within the O-ring seal during all etching processes. The HF concentration of the electrolyte was 1 M.

The sample was etched under different conditions (see Table 1). In Fig. 13a the result of such an etching process is shown. UV illumination results in different etching of p-type and n-type regions. Both the n-type substrate and p-type region were etched using a reference bias V_{ref} vs. the Pt reference electrode between −0.15 V and −0.12 V. The porosity of the surface is visible in all the profilometer measurements. The etched step in the n-type substrate is about 0.6 μm deep; the surface is rough with pillars up to the former surface. The etched depth in the implanted p-type region is 1.0 μm and shows no such pillars. The difference in depth between the implanted region and the substrate of 0.4 μm is nearly the same as the depth of the implanted p-type region. Therefore, the p-type region is obviously etched prefentially. Furthermore, one can observe a kink in the etched region at the level of the p-n junction (depth of about 0.45 μm), which could be marked by this method obviously.

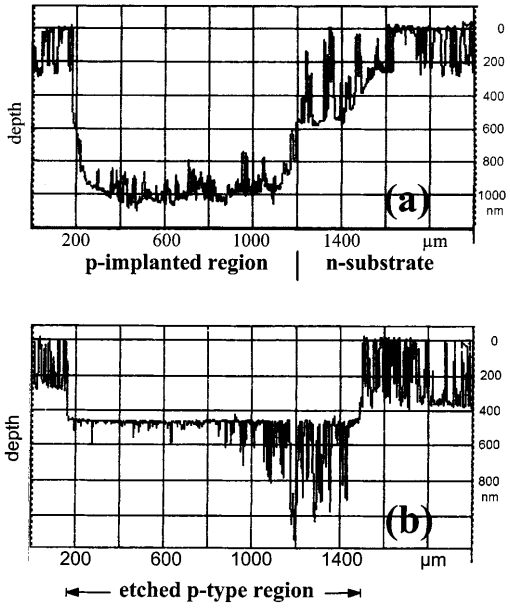

Fig. 13a, b Profilometer measurements of the etched depth of ion implanted p-type structures in n-type substrate after the etching process. **a** $V_{ref} = -0.15$ V; etching time: 10 min. The p-type region (thickness 0.5 μm) vanished completely; the underlying n-type substrate is also etched. The n-type substrate next to the former p-type region is etched (*right*). **b** $V_{ref} = +0.20$ V; etching time: 20 min. Only the p-type region is etched and an etch stop can be observed at the p-n junction

Using a reference bias V_{ref} between +0.15 V and +0.20 V the n-type substrate is not markedly etched in contrast to the p-type region. The etched depth of the p-type region is 0.45 μm in all our experiments, showing a very planar bottom (Fig. 13b), although the etching time varies between 2 and 20 min (see Table 1). We conclude therefore that, there is an etch stop. Without UV illumination, no etching occurs; the UV illumination is a necessary for the etching processes described above.

n^+np^+-mesa diodes

The preparation process of the n^+np^+-mesa diodes is identical to the p^+pn^+-mesa diodes: CVD epilayers and RIE. The doping concentrations of the n-type layer and the p^+-epilayer are 2.4×10^{15} cm^{-3} and 1×10^{19} cm^{-3}, respectively (see Fig. 10b). Every etching process on n^+np^+-mesa diodes was conducted under UV illumination with a HF concentration of 1 M. Table 2 shows the different parameters of four etching processes. Process number 2 results in a rough and porous surface, which is similar to regular etching of n-type material. Processes number 3 and 4 end up with an etch stop. The

Table 2 Etching results of the n^+np^+-mesa diodes with UV illumination

V_{ref} (V)	Etching time (min)	Etched depth of the n-type base (μm)	Result
+0.20	5	0.3	preferentially etched p-region
+0.17	20	0.5	porously etched
−0.18	10	0.2	etch stop
−0.27	20	0.1	etch stop

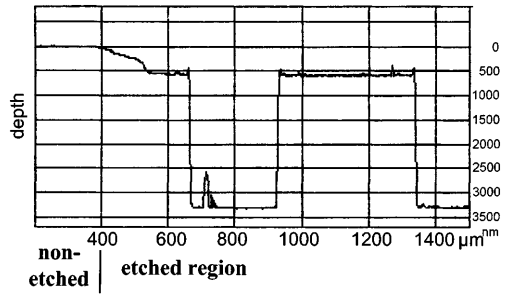

Fig. 14 Profilometer measurements of the etched depth of n^+np^+-mesa diodes after the etching process. The p-type epilayer (thickness 0.6 µm) has vanished at the right mesa diode. At the p-n junction an etch stop occurred. On the left diode the O-ring has prevented any etching

p^+-epilayer within area of the O-ring seal has vanished (see Fig. 14). The heights of the mesa diodes are reduced by 0.6 µm, which is equal to the thickness of the p^+-epilayer. The n-substrate base is also etched, but only by about 0.1 µm–0.2 µm.

Discussion

Two different geometries of p-n junctions were realized and examined. In contrast to results reported in the literature [5, 6], the substrate itself is contacted and not the epilayer. Using a n-type layer on a p-type substrate, only the p-type substrate is etched. For the etching process of a p-type layer on a n-type substrate, the p-n junction operates in reverse bias and UV illumination is necessary. The electron-hole pairs produced by the UV illumination are separated in the space charge region of the p-n junction. The electrons are transported to the back side contact, the holes can tunnel to the surface and electrochemical etching can occur (see Fig. 15). The tunnelling of the holes is promoted by the relatively high p-type doping concentration, resulting in a strong band bending and a narrow space charge region at the surface.

The reason for the high selectivity in the etching of p-type layers on n-type substrates, and particularly for the observed etch stop under UV illumination, is not completely understood. We suppose the weak band bending of the relatively low n-doped substrate plays an important role.

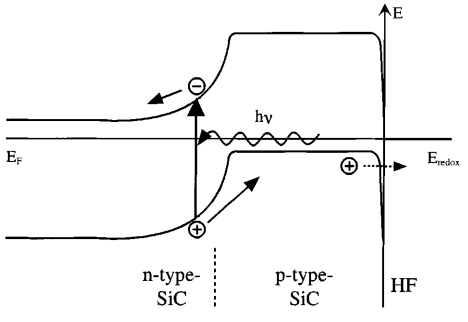

Fig. 15 Energy band diagram of a p-type-SiC/n-type-SiC/electrolyte structure without any applied voltage. The UV illumination generates an electron-hole pair, which is separated in the space charge region of the SiC. The hole is tunnelling to the surface

Results on 6H-4H heteropolytype junctions

The investigated sample was grown by the modified Lely method using two Acheson seed crystals side by side (both C-face up, one "on-axis", the other 8° "off-axis" oriented). This method enables the simultaneous growth of 6H-SiC and 4H-SiC [15]. The prepared sample this way is n-type with a doping concentration of 2×10^{17} cm^{-3} for both polytypes. The etching processes were made under UV illumination with 1 M electrolyte solution.

To compare the photoelectrochemical properties of the different polytypes, current-voltage measurements were conducted separately for the 4H-SiC and the 6H-SiC region using an O-ring with an inner diameter of 1.78 mm (Fig. 16). The slopes of the *j-V* curves and the saturation currents were nearly equal (Fig. 17). The intersections of the voltage axis with the extended linear region of the curves determine the "threshold" voltages; shifts of the "threshold" voltage from −0.59 V for 4H to −0.37 V for 6H were observed.

During the etching processes of the 6H-4H heteropolytype junction an O-ring with an inner diameter of 3 mm was also used. The sample was located in such way that both polytypes were exposed to the electrolyte solution (Fig. 16). The parameters of the two etching processes are shown in Table 3. An etching of only the 4H region could be observed in both cases. This means that the 6H-4H heteropolytype junction is marked. The optical microscope image in Fig. 16 shows the etched 4H region with a grey colour different from the smooth non-etched 6H region. Figure 18 shows the depth profiles resulting from two etching processes using different bias voltages. The 6H-4H junction is revealed by a sharp step at a bias of $V_{ref} = +0.10$ V; the etched depth is up to 1.5 µm after an etching time of 8 min. Using a lower bias of $V_{ref} = -0.45$ V the etched 4H region is strongly porous with a depth of only 0.2 µm after 8 min.

Discussion

The shifts of the current-voltage curves of the 4H-SiC and the 6H-SiC in Fig. 17 are determined only by the different polytypes, since the same growth conditions produce identical crystal quality and doping concentration. Thus the shift of 0.22 V of the threshold voltage between 6H-SiC and 4H-SiC represents the difference in the n-type flatband voltage, which is almost identical to the excitonic band gap difference of 0.23 eV between 6H-SiC (3.00 eV) and 4H-SiC (3.23 eV) [16], resulting in the conclusion that the total band offset between 6H- and 4H-SiC is nearly completely due to a shift of the conduction bands.

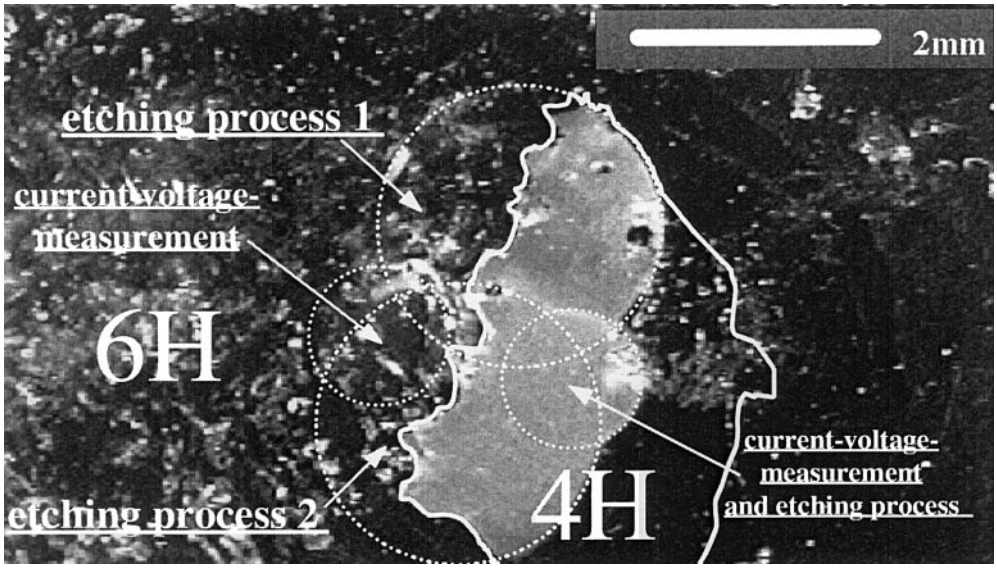

Fig. 16 Light microscope picture of the 6H-4H sample with the etched 4H-region (light grey) and the drawn-in position of the O-rings (dotted circles)

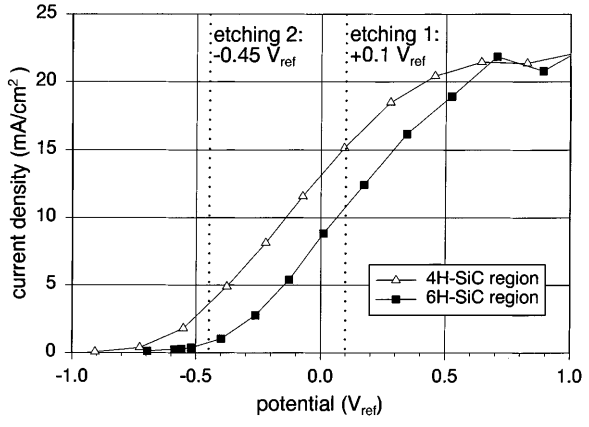

Fig. 17 *j-V*-characteristics of the 6H-SiC and the 4H-SiC region of the 6H-4H sample ($N_D = 2 \times 10^{17}$ cm^{-3}) in 1 M HF. The dotted lines represent the etching voltages

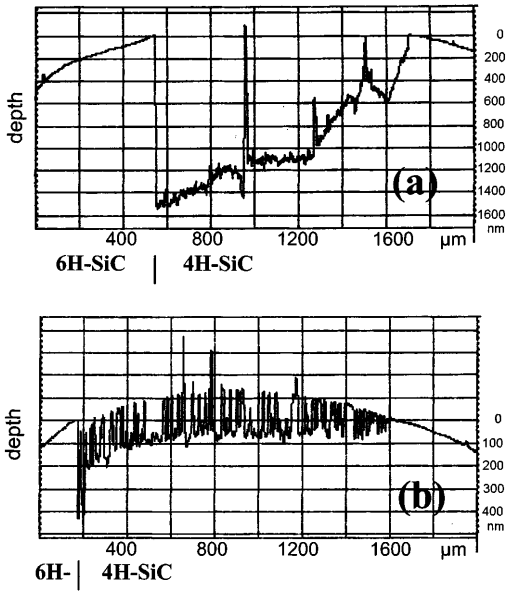

Fig. 18a, b Profilometer measurements of the etched depth of the 6H-4H region after the etching process. Only the 4H region is etched. **a** $V_{ref} = +0.10$ V; etching time: 8 min **b** $V_{ref} = -0.45$ V; etching time: 8 min

Table 3 Etching results of the 6H-4H-SiC sample

V_{ref} (V)	Etching time (min)	Etched depth of the 4H region (µm)
+0.10	8	up to 1.5
−0.45	8	0.2 (porous)

In Fig. 17 the values of the applied etching voltages are indicated as dotted lines. At both voltages the current densities through the 4H region is significantly higher than the current densities through the 6H region. At $V_{ref} = -0.45$ V the current for 6H-SiC is nearly zero; thus, only etching of 4H-SiC is possible; at $V_{ref} = +0.10$ V, however, the current for 6H-SiC and 4H-SiC differs only by a factor of 1.5. Since the observed etching is selective for different polytypes, the hole transport to the 4H-SiC and the 6H-SiC regions does not behave like in a parallel resistance network.

Appendix: anodic oxidation of SiC

To realize an anodic oxidation and not an etching of SiC, the electrolyte HF has to be substituted by HCl; then the SiO_2 layer (see Eqs. 1 and 2) is not removed. The samples we have oxidized were n-type 6H-SiC. The oxidation was carried out with a HCl concentration of 0.20 mol/l under UV illumination and an inner diameter of the O-ring of 1.78 mm. After the oxidation process a height gain of several µm was observed (Fig. 19). The oxidation parameters and experimental results are summarized in Table 4.

One of the oxide films was investigated by Rutherford back scattering spectrometry (RBS) under a scattering angle of 168° with a 2 MeV He^+ beam for a stoichiometry determination (Fig. 20a) and with a 2 MeV H^+ beam for achieving depth information (Fig. 20b). Figure 20a shows that the stoichiometry of the oxide

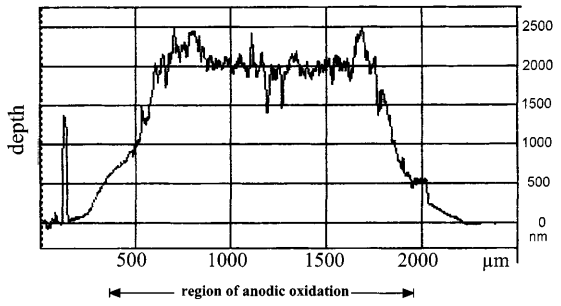

Fig. 19 Profilometer measurement of the height of the anodic oxidized SiC. The oxide has caused a height gain up to 2.5 µm to the former surface. Oxidation time 60 min, flow charge 134.2 mC

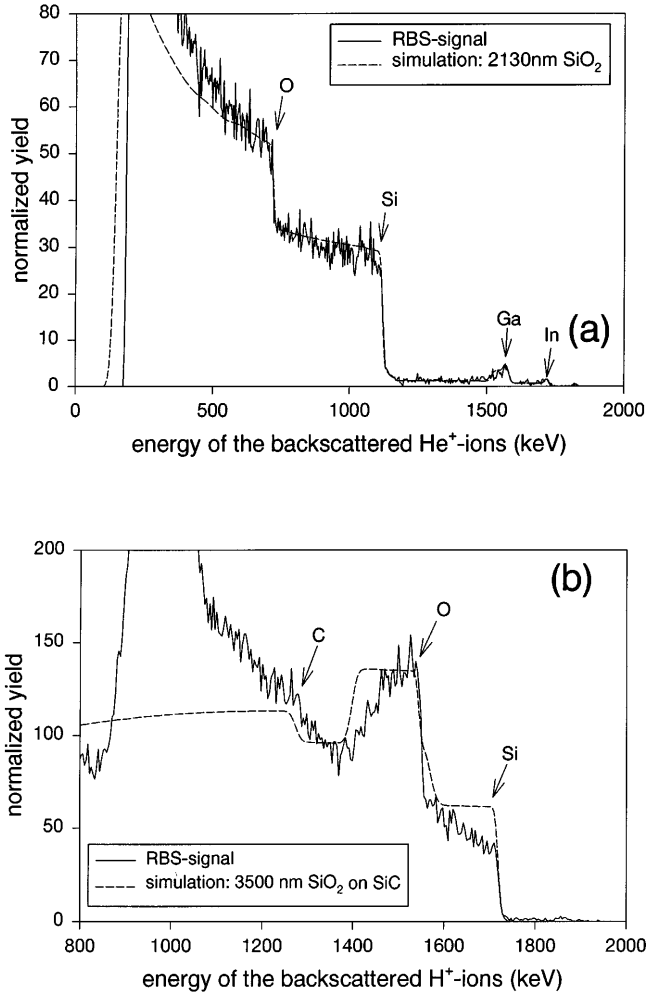

Fig. 20 RBS spectra of the oxide of an anodic oxidized SiC sample (same as in Fig. 19) with simulations to the curves (dashed lines) for **a** He^+ ion beam and **b** H^+ ion beam

Table 4 Results of the anodic oxidation of a n-type substrate

N_D (cm^{-3})	Oxidation time (min)	Flow charge Q (mC)	Height of the mesa structure (µm)
1.3×10^{18}	110	361.9	4.5–5.0
1.9×10^{18}	60	134.2	2.0

layer is in good agreement with the result of a numerical simulation assuming a SiO_2 density of 1.65 g/cm^3 including impurities of Ga and In (total amount $<1.5\%$). Using a H^+ beam (Fig. 20b) the oxide thickness of the film turns out to be between 3 µm and 4 µm, showing a gradual transition from the oxide to SiC, which can be seen by the decreasing O plateau (towards low energies) and increasing Si plateau (towards high energies). However, the surface of the oxide is rough with cracks, possibly caused by the volume expansion of the oxide, with an increasing diameter of the mesa structure towards the bottom, which is due to the increasing diameter of the O-ring near to the bottom.

Acknowledgements The 6H-4H samples were grown by V. Hydemann and N. Schulze in our laboratory and SiC crystals were bought from Cree Research. The mesa diodes were kindly supplied by J. P. Chante and S. Ortolland from INSA in Lyon.

References

1. Jepps NW, Page TF (1983) Prog Cryst Growth Charact 7: 259
2. Wolf R, Helbig R (1996) J Electrochem Soc 143: 1037
3. Yih PH, Saxena V, Steckl AJ (1997) Phys Status Solidi B 202: 605
4. Münch W v (1982) In: Madelung O, Schulz M, Weiss H (eds) Landolt-Börnstein New Series III vol 17., SiC, Semiconductors, Springer-Verlag Berlin Heidelberg, p 414
5. Shor JS, Osgood RM, Kurtz AD (1992) Appl Phys Lett 60: 1001
6. Shor JS, Kurtz AD, Grimberg I, Weiss BZ, Osgood RM (1997) J Appl Phys 81: 1546
7. Shor JS (1995) Properties of SiC. INSPEC, The Institution of Electrical Engineers, London, pp 141–149
8. Brander RW, Boughey AL (1967) Br J Appl Phys 18: 905
9. Stein RA, Rupp R (1994) In: Spencer MG et al. (eds) Inst Phys Conf Ser vol 137 Electrolytic etching of Silicon carbide, Silicon carbide and related Materials, IOP Publishing, Washington, p 561
10. Lauermann I, Meissner D, Memming R, Reineke R, Kastening B (1991) In: Winsel A (ed) Dechema Monographien vol 124. Wasserpaltung an und Stabilisierung von SiC in wäßrigen Lösungen, Elektrochemie in Energie- und Umwelttechnik, VCH, Weinheim, p 617
11. Verhaverbeke S, Teerlinck I, Vinckier C, Stevens G, Cartuyvels R, Heyns MM (1994) J Electrochem Soc 141: 2852
12. Gerischer H (1978) J Vac Sci Technol 15: 1422
13. Shor JS, Osgood RM (1993) J Electrochem Soc 140: L123
14. Shor JS, Kurtz AD (1994) J Electrochem Soc 141: 778
15. Heydemann VD, Schulze N, Barrett DL, Pensl G (1996) Appl Phys Lett 69: 3728
16. Choyke WJ (1990) In: Freer R NATO ASI Ser vol 185. Physics and chemistry of carbides, nitrides and borides, Kluwer, Dordrecht p 563